# PARAMETER-FREE, PREDICTIVE MODELING OF SINGLE EVENT UPSETS DUE TO PROTONS. NEUTRONS, AND PIONS IN TERRESTRIAL COSMIC RAYS

G.R. Srinivasan, H.K. Tang, and P.C. Murley Semiconductor Research and Development Center, IBM East Fishkill, Hopewell Jct., NY 12533

## **ABSTRACT**

In this paper we present a new approach and a computer software for modeling single event upsets. This model, named Soft Error Montecarlo Model (SEMM), does not need any experimental inputs or any parameter fitting. It is intended to be a design tool for chip designers when they want to optimize their designs for soft error hardness and performance. The paper focuses on terrestrial cosmic rays that cause single event upsets. Details of the nuclear modeling and of the coupled device-circuit modeling are presented. Also presented are the comparison of SEMM predictions against measurements of single event upset rate in proton beam experiments and in computer main frame field tests performed at high ground elevations. We also present some proton-pion comparisons that are relevant to single event upsets.

## I. INTRODUCTION

It is well-known that both primary and terrestrial cosmic rays generate a considerable number of single event upsets (SEU) in modern integrated circuit (IC) chips in both the space environment and at aircraft altitudes. But their occurrence at ground level is being reported only recently [1]. This tend-ency for SEU can get worse as the chip technology moves to lower critical charges and operating voltages. Although there are many defense measures in terms of technology, circuit, and system changes that one employs to overcome the soft error reliability problems, it is, nevertheless, very useful to know the single event upset rate (SEU rate) at the design stage of a chip, so that many options can be evaluated and traded-off against performance and cost. It is with this objective we have developed a simulation tool, called SEMM. We have reported recently some preliminary results of this model, especially from a chip reliability point of view [2]. It is the purpose of the present paper to examine the model for cosmic ray applications in some detail, including some new pion calculations and first time results of experimental measurements vs. predictions for protons and terrestrial cosmic rays for both bipolar and CMOS chips. One of our goals in developing this model was to make the model predictive, without any need for arbitrary fitting parameters. In that spirit, we approach the problem from nearly first principles and use the state-of-the-art simulations of nuclear spallations and device and circuit behavior. As an important departure from many previous studies on the calculation of the SEU rate, we use the full treatment of the chip circuitry as opposed to the simulation of a few devices in the chip. We also use full 3D chip geometry, so that any complicated chip can be simulated. For this, we need to know the full chip layout at all mask levels, and,

dopant profiles. There are no built-in default values for these inputs. The computer software SEMM has been tested with many experiments, and is used routinely in IBM for the design of CMOS and bipolar chips.

## II. BRIEF SUMMARY OF PREVIOUS WORK

Modeling of the SEU rate for aerospace applications is usually made without a detailed chip topology and circuit information. Methods are therefore developed to characterize the chips in terms of particle accelerator experiments and charge collection experiments. Many excellent reviews may be found in the literature on these methods [3-5], and we limit our discussion here to a few salient points. These methods rely on the estimation of sensitive volume and critical charge pertaining to a chip. High-energy, heavy ion beam experiments are generally used to obtain this information. Since the experiment is based on the entire chip exposure to the beams, considerable difficulty exists to associate these parameters to individual devices in the chip. Thus, it is often not possible to take into account the variations of these quantities from device to de-This becomes very important when dealing with IC chips which have different types of junctions with varying extents of funneling and diffusion contributions to charge collection. Use of the burst generation rate method (BGR) [6], together with the rectangular parallelpiped (RPP) approximation [7] of the sensitive volume, allows an estimation of SEU rate due to protons and neutrons. The nuclear models needed for this purpose have improved since the original BGR approach (see for example [8,9]), but the basic limitations of the BGR method still remain. Computation codes, such as CUPID [10], are also used for this purpose. One of the main requirements for a SEU rate predictive tool that is independent of experiments is the ability to calculate the critical charge and the sensitive volume and their variations within a chip.

From a device/circuit simulation point of view, there have been 2D and 3D device simulations for determining the SEU rate [11,12]. In these simulations the transport and collection dynamics of excess carriers generated by the radiation events are modeled for specific devices. Several recent treatments [13-15] have also included some circuit aspects in the simulation. Yet, for a full chip simulation a completely coupled device-circuit analysis is needed. Also, as we see later, the chip response changes from one event to another event of the same kind because of the current wave form effects. Averaging these effects may introduce large errors in the SEU rate calculation. It is thus necessary to simulate the SEU on an event by event basis. It is also necessary to treat simultaneous charge collection at different nodes that is caused by the generation of multiple

0018-9499/94\$04.00 © 1994 IEEE

tracks in cosmic ray hits. These effects have been modeled in SEMM.

#### III. THE MODEL

#### (i) Simulation Methodology

The methodology used in SEMM is illustrated in Fig. 1. The left half of the figure shows the tools and information necessary to set up the charge collection history files which record the amount and arrival times of the charge packets. This is done for all the sensitive nodes in the analysis region. The analysis region is defined as follows. The repetitive

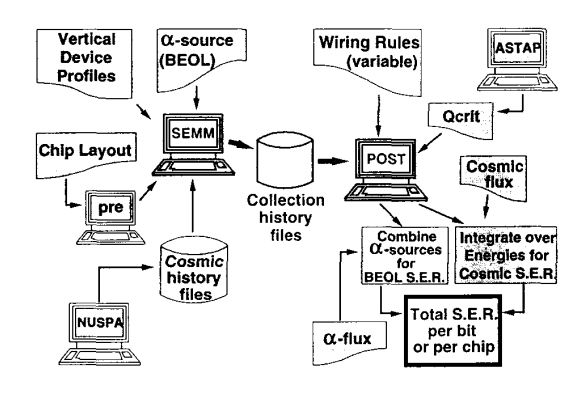


Fig.1. SEMM Flow chart

sections of the chip, which we call lots, are input from the chip layout into SEMM through a preprocessor. After the coordinates of the hit are selected at random, SEMM forms an analysis region consisting of many lots within which all the tracks produced by the hit can be projected. Within these lots all device regions and oxide and insulating regions are represented. Figure 2 shows a typical lot for a bipolar logic chip.

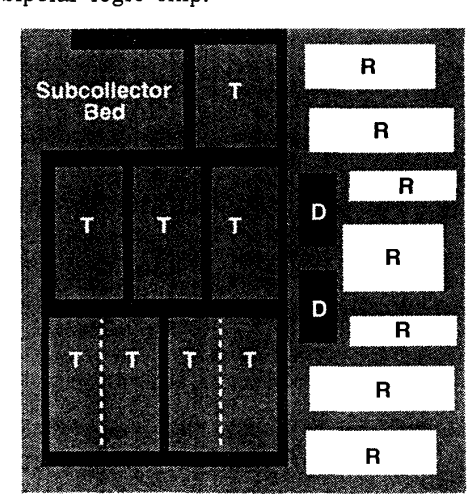


Fig.2. A SEMM lot for a bipolar logic chip. T, R, and D are transistors, resistors, and Schottky diodes respectively.

SEMM also calls for vertical dopant profiles in order to calculate the built-in field and the electron-hole recombination rate.

The radiation sources are handled through subroutines describing the individual metal lines, solder contacts, etc., which generate chip alpha particles. For cosmic ray applications a separate nuclear spallation simulator (NUSPA) is used as the radiation source. We will describe NUSPA in more detail later. The chip alpha radiation sources produce events of known energy from the assumed or measured radioactive energy spectra. We have measured and compiled the flux and the energy spectra of the alpha particles emanating from metal layers, ceramic packaging, and solder contacts which we use in SEMM. SEMM calculates the energy attenuation within the source and in the intervening From the known stopping power of alpha lavers. particles in silicon [16] track lengths and the number of electron-hole pairs produced per unit length are calculated. In describing these tracks we do not use constant linear energy transfer (LET) assumptions that are often used in SEU modeling, and we allow for the changes in the stopping power along the ion track. The position and angle of these tracks relative to the chip geometry are picked randomly. Since each of the sources is treated separately, their contributions can be summed up. The cosmic ray history files supply records of tens of thousands of proton and neutron hits on the chip nuclei for each energy using NUSPA. Each record has the type, kinetic energy, and the directions of the ions produced due to spallation. A separate file is created which records the consequences of elastic collisions using optical potential simulations [17]. Again, this elastic history file has energies and directions of nuclear elastic recoils. SEMM uses both these files for each energy of the proton or neutron hit according to the theoretical ratio of elastic to inelastic nuclear cross sections. The SEMM program selects randomly a nuclear event of proton or neutron collision from these files, and, from a table lookup of the energy loss and electron-hole pair production for different ions produced in the collision, forms the multiple tracks relative to the chip axes. Again, as in the alpha case, the position of the hit is selected randomly. In order to simulate the azimuthal variation in the intensity of the terrestrial cosmic rays, we have provided a cosine power law which weights the random selection.

Once the tracks due to a proton or neutron collision are set up, together with the variation in charge density along the tracks, SEMM divides the tracks into small segments, each with a packet of charge of about 1000 electron-hole pairs, and looks up the positional code for each mesh region containing the packet. An electron-hole pair from this packet is allowed to diffuse and be collected by the device junction or recombine. This pair represents the transport and collection of all the electron-hole pairs in the charge packet. This methodology was developed by Sai-Halasz [18] for random walk treatment of the charge transport to save considerable amount of computer time and memory, and we use that technique in SEMM. We examine the details of the device and circuit modeling in a later section.

Since SEMM allows for the collection at all the junctions in the chip analysis region, these charge values are saved in the collection history files, together with their time of arrival at each junction. This is a large file and uses considerable amount of memory space, typically of the order of several megabytes. The right portion of Figure 1 is the post-processing of the charge history files through a circuit analysis program (ASTAP in the figure) and a circuit model for the chip. The rest of the post-processing is to combine the alpha particle induced SEU rate with the alpha particle flux as determined separately for these sources. For cosmic ray calculations, the cosmic ray flux data (proton and neutron flux vs. energy) is integrated with the SEU rate per proton or neutron as calculated by SEMM for several chosen energies to give the total SEU rate for the chip.

## (ii) Nuclear Modeling

## (a) Case of Protons and Neutrons:

Central to the modeling of SEU due to protons and neutrons is the ability to model accurately the elastic and inelastic scattering of these particles with the chip nuclei, such as silicon and oxygen. We have paid considerable attention to this problem, and some of this work has been reported before [19,20]. Recently we have extended the modeling work to pion-silcon reactions which we report in the present paper. The basic methodology we chose to model nuclear spallation follows that of Bertini's original work (MECC) [21], i.e., the cascade-statistical approach. In this approach the spallation takes place in two stages: the nuclear cascade stage where the incident proton or neutron enters the target and suffers binary collisions with the protons and neutrons in the target nucleus as specified by the free nucleon-nucleon cross sections. The energy states of the nucleus, Fermi motion of the nucleons within the target, and the Pauli principle dictate the outcome of the Monte Carlo simulation of the cascade process. At the end of the cascade stage, one or more nucleons may leave the system, mostly in the forward direction. The remaining nucleus is an excited compound nucleus which undergoes a

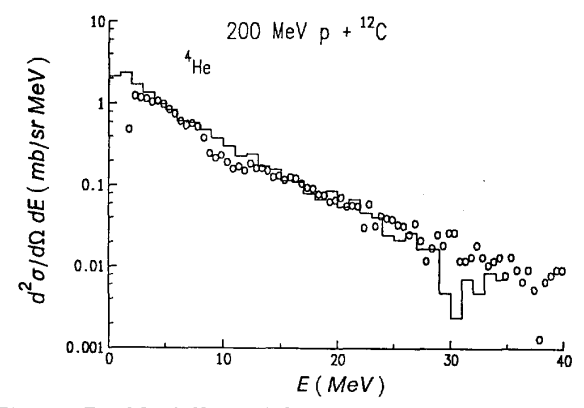


Fig.3. Double-differential alpha particle production cross section vs. energy for 200 MeV protons incident on carbon. Circles are experimental measurements and the histogram is due to NUSPA.

statistical decay to achieve thermodynamic equilibrium. A new statistical code which takes into account the proper inverse capture cross sections of the emitted particles and all exit channels was written in NUSPA. With these modifications NUSPA predicts the proton and alpha cross sections much better than MECC. The entire model is extensively tested with a large data base. As an example, we show two figures (Figs. 3 & 4) where the double differential production cross section vs. the energy of alpha particles for 200 MeV protons incident on carbon (Fig.3), and the double-differential production cross section vs. energy of neutrons for 800 MeV protons incident on aluminum are shown. It is to be pointed out that the double differential cross

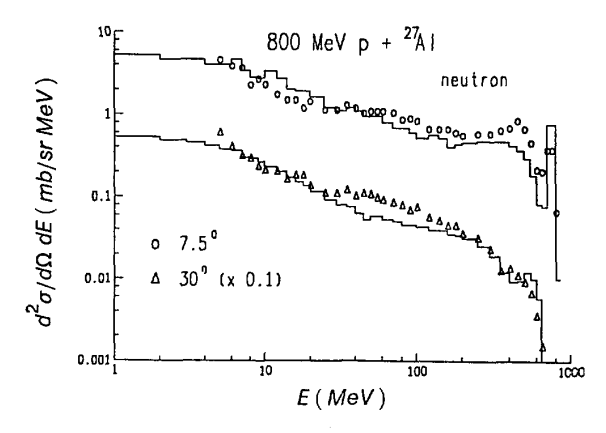


Fig.4. Double-differential neutron production cross section vs. energy for 800 MeV proton incident on aluminum. Histograms are NUSPA results.

section is a stringent test for the nuclear model, and NUSPA reproduces the data very well.

NUSPA has several unique features. It generates absolute cross sections such that direct comparison with experiments is possible without any arbitrary normalization. All exclusive reaction channels are included. Also, the model obeys the fundamental sum rules, which gives a good description of the recoil distributions that are important for SEU rate calculations. Finally, the model gives the kinematics of individual events, so that one can construct a spallation history file, as mentioned before. We note that since NUSPA is a Monte Carlo model, the same incident event could produce totally different kinematic results the next time. In Table 1 we show a typical history file for 3 cases of a 150 MeV proton colliding with a silicon nucleus. In the first case, 1 proton, 4 neutrons, 3 alpha particles, and a carbon residual nucleus are produced. (We have not shown the lighter nuclei such as deuterons and tritons in this table, and both He3 and He4 isotopes are counted as alpha particles.) The second and third cases produce very different products. Since we know the kinetic energies and the directions of these emitted particles, we can set up their tracks in a silicon chip as described before. For most practical purposes we can neglect the secondary protons and keep only the residual nuclei and the alpha particles, if any. Figure 5 shows the NUSPA calculated energy spectra of the recoil

nuclei and of the alpha particles for two incident proton energies.

Residual Nucleus	Туре		MeV	Angle Cosines		
_	12	6	8.15	0.6225	0.2480	0.7423
	n		44.07	-0.1785	-0.3052	0.9354
ļ	l p		1.26	0.8576	-0.4737	-0.2002
ŀ	'n		12.42	-0.1210	0.8615	-0.4931
12 C 6	n		16.90	0.4377	-0.0547	0.8974
1,20	n		3.34	0.4671	-0.8534	-0.2312
'2	alp	ha	11.04	-0.6426	-0.5151	-0.5672
	alpha		3.57	-0.8732	-0.0248	-0.4868
	alpha		4.12	-0.3110	-0.4230	0.8511
<sub>27</sub> Al <sup>13</sup>	27	13	2.73	0.9830	0.1800	-0.0359
AI	р		84.07	0.6399	0.3677	0.6748
27	p		52.82	0.3255	-0.2590	0.9094
	26	13	0.18	0.7500	-0.6612	-0.0186
<sub>26</sub> Al <sup>13</sup>	'n		134.88	0.1033	-0.1580	0.9820
26 A1	n		3.08	0.4502	-0.1419	0.8816
	n		1.71	-0.8699	-0.1911	-0.4547

**Table 1.** Nuclear spallation history file events for 150 MeV protons incident on silicon.

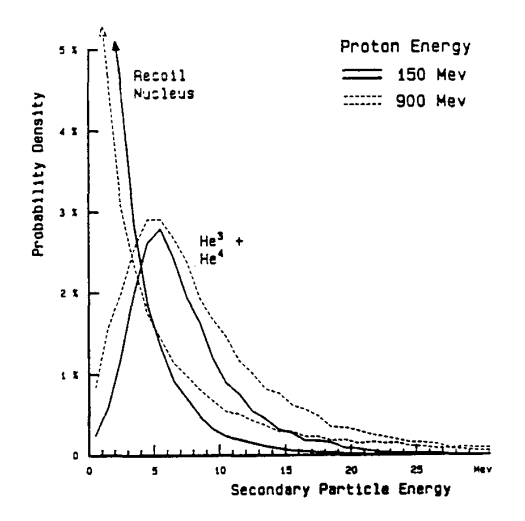


Fig.5. Energy spectra for the recoil nuclei and alpha particles for two incident proton energies.

We note from the figure that most of the recoil energies are below 5 MeV, and the alpha particles have long, high energy tails. The result of this event-by-event treatment is to allow the simulation of simultaneous, multiple tracks in the chip. Since, depending on their angles and range they intersect different parts of the collecting regions of several junctions, different current wave forms (pulse shapes) are produced by different events of the same kind. We discuss the consequence of this result in a later section on device-circuit modeling.

We now consider elastic collisions. In the SEU literature many calculations have been made considering the energy deposited by elastic recoils. In an elastic event no energy is lost to the internal excitations of the target nucleus. The elastic collisions are mostly forward-peaked, with the energy transfer falling off rapidly with the angle from the incident direction. The elastic events are analyzed

using standard proton- and neutron-nucleus optical potential models [17]. Using the variation of the elastic cross sections with the angle for both the incident particle and the recoil nucleus, and using standard kinematic considerations, one can reconstruct a history file similar to the case of spallations. In the elastic case we need to consider only the recoil nucleus track, since the incident particle is still moving too fast to have any appreciable energy loss in the medium. While the elastic cross section predominates in the total (i.e., elastic + spallation) scattering cross section at very low projectile energies, the probability of occurrence of elastic recoil energies greater than 1 MeV is very small. It is typically an order of magnitude or more smaller than the similar number for spallation. At higher energies, greater than 100 MeV, the cross section for elastic recoil of energies larger than 1 MeV is still small. The elastic contribution to SEU rate becomes significant only for chips with very low critical charge and at very low proton and neutron energies for which the elastic scattering cross sections are much higher than the spallation reaction cross sections.

## (b) The case of Pions:

Besides protons and neutrons, pions occur in terrestrial cosmic rays and cause strong (nuclear) interactions with elemental nuclei. But their abundance at sea level is two orders of magnitude below that of neutrons in the energy range of interest. However, their flux becomes appreciable at higher altitudes, and thus one would like to know their effects on the SEU rate of IC chips. We have extended NUSPA to make the calculations of the distributions

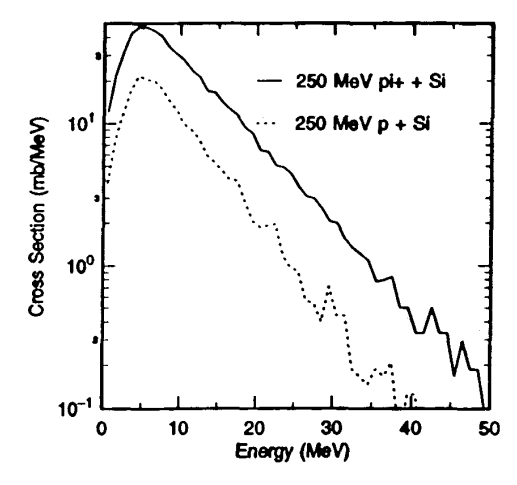


Fig.6. Helium energy spectra for 250 MeV pion and proton reactions with silicon.

of secondary alpha particles and heavy recoil nuclei due to pion-silicon interactions. It should be pointed out that, due to the fairly large deBroglie wavelength of pions at low and moderate energies (100 - 1000 MeV), the semi-classical picture of the cascade stage is only approximate. Also, the formation of quasi-bound pion-nucleon states (called delta resonance) inside the nucleus complicates the model. We have, nevertheless, run NUSPA with appropriate

free cross sections and have obtained a reasonable agreement (to within 20%) with the experimental measurements of reaction cross sections. Since our interest is SEU rate modeling, we compared the pion and proton reactions with silicon. Figures 6 and 7 show this comparison. Figure 6 shows the energy spectra for the helium nuclei in 250 MeV proton and pion collisions with silicon. Figure 7 shows similar results for the recoil nuclei. We see from both

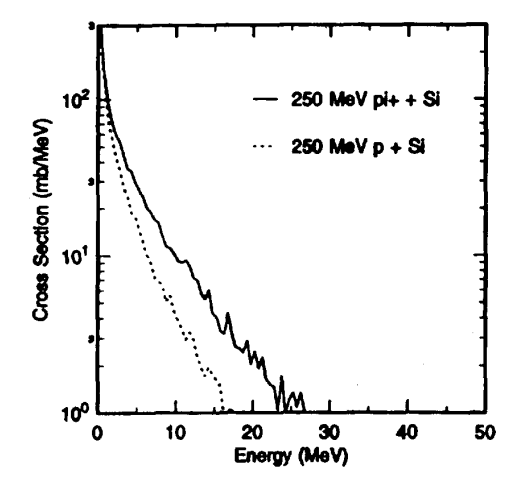


Fig.7. Excitation spectra for the recoil nuclei in 250 MeV pion and proton collisions with silicon.

these figures that both the helium and recoil cross sections are larger for pions than for protons at all energies of the spectrum. This difference, however, narrows down when the projectile energy approaches 750 MeV. One interpretation of this higher cross section for the pion case is the occurrence of delta resonance. The consequence of this finding is that, although the pion flux in the terrestrial cosmic rays is low, the

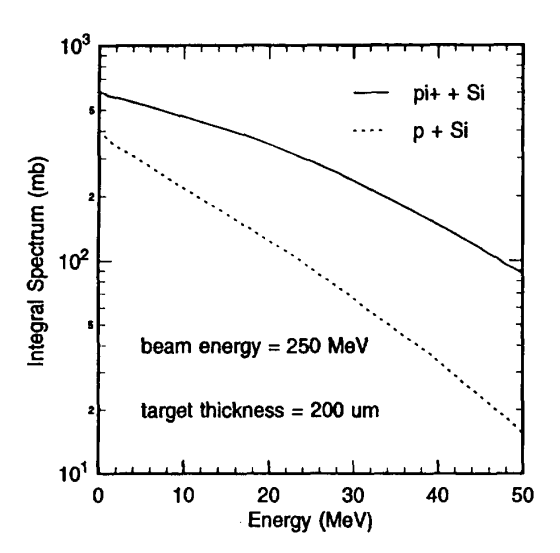


Fig.8. Energy deposition by pions and protons at 250 MeV in a 200  $\mu$  m silicon slab.

pion effect on the SEU rate may be significant, especially at higher altitudes. We followed this study of pions with a calculation of the energy deposition in a thin (200  $\mu$  m) slab of silicon from secondary ion fragments generated by the 250 MeV pions and protons. This is shown in Figure 8 where the integral cross section, plotted on the y-axis, is proportional to the total deposited energy greater than E shown on the x-axis. The figure shows that pions deposit more energy in silicon than protons at 250 MeV. The calculation of SEU rates for IC chips due to atmospheric cosmic ray pions is in progress and will be reported later.

## (iii) Device and Circuit Modeling

The electron-hole transport methodology has been described adequately before [2], and we describe only the highlights here. The Monte Carlo technique for charge transport is based on the premise that the steady-state device fields are negligibly perturbed by the excess carriers produced by the ion tracks. SEMM treats the ionization to be instantaneous and assumes that the track width is less than the smallest mesh spacing. The Monte Carlo treatment of the charge transport and collection has several advantages. It allows a treatment of a large number of devices connected in an IC chip as specified in the chip design. The diffusion is performed by random walk, the steps of which are modified by local fields. A transient device simulation is only necessary to determine the general shape of the current pulses as collected by various junctions. SEMM determines the actual pulse shape at each junction by fitting its charge vs time history to the expected general shape. This shape varies with the extent of funneling and diffusion present in the charge collection at any given junction. We use a double exponential pulse shape [2] to fit the SEMM pulses with a characteristic rise time (1 ps) and a varying decay time.

In a simulation, which involves a circuit response to current pulses, one has to have a coupled device-circuit model for that particular chip. All chip designs have their circuit models where the circuit parameters are obtained through either parameter extraction from the device models and model generation programs or through empirical I-V curves. This circuit model can then be used to study the effect of disturb currents of a given shape injected at various sensitive nodes to obtain the circuit response. A circuit simulator (eg. ASTAP or SPICE) is used to make the analysis. The parameter that is of interest for the SEU rate calculation is the critical charge. This is a circuit parameter obtained by studying the response of the circuit to current pulses of different shapes and total charge. The lowest charge that is necessary to change the state of the circuit is the critical charge for that particular current pulse shape. A library of these critical charges vs pulse decay time constant is made and stored in SEMM for determining whether a particular SEMM pulse from a junction caused an upset or not. This methodology of coupled device-circuit modeling obviates the need for running device simulations for each case. It should be mentioned that a major parameter that influences the critical charge is the cell's bias current. This can vary from

place to place on the chip due to both resistive drops in the word and drain lines and due to temperature variations across the array of cells. It can also vary from chip to chip due to variations in the manufacturing process parameters and due to variations in the chip power supply voltages. These variations can be considered when the critical charge is calculated as a function of typical cell standby current. The chip designer will supply these changes as variations in the critical charge numbers to SEMM for soft error calculations.

With this approach adopted in SEMM, SEU is determined for each event and is repeated thousands of times to build up statistics. The method also allows the calculation of the SEU rate produced by multiple tracks which are simultaneously formed in a cosmic ray hit. Figures 9 and 10 demonstrate the effect of pulse shape on the response of a chip, where a pulse with a time constant of 0.1 ns causes a change of state, while pulses of the same total charge (485 fC), but with time constants of 0.3 and 0.5 ns do not. I.e., the critical charge for a 0.1 ns pulse is close to 485 fC, whereas 0.3 ns and 0.5 ns pulses have critical charges larger than 485 fC. It should also be noted that if the charge collected is very close to the critical charge for that pulse, the circuit takes a long time to switch and can remain in a metastable state until switching occurs due to some stray noise in the circuit.

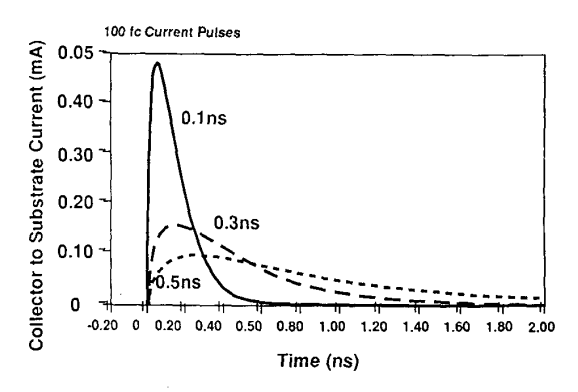


Fig.9. Pulse shapes for three time constants and same total charge.

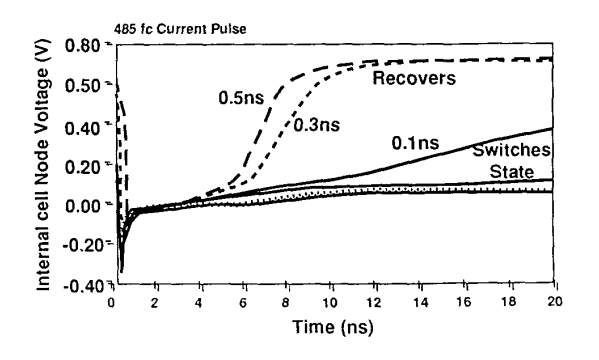


Fig.10. Circuit response to the three pulses of same total charge (485 fC) with three different time constants.

One of the effects that we need to simulate properly is the effect of charge sharing by different nodes. SEMM charge collection procedure allows a determination of the current shape and the charge stored by neighboring nodes. Their effect is obtained only through the circuit analysis using the particular chip circuit model. We have experimented by applying currents at various neighboring nodes to determine if and how the partial critical currents add. We have found, for example, by applying 50% of the critical charge at a high node in a CMOS SRAM cell and applying a nearly 50% critical charge at the low node in the opposite direction, we can cause a cell upset. These experiments have led us to conclude that the partial currents and charges can be summed by linear superposition. The criterion for failure is then that an upset occurs when the sum of the ratios of the actual charges collected by neighboring nodes divided by their respective critical charges is equal to or greater than one. This way we can include all the charge sharing effects in our simulation.

One other effect that is important, especially in aircraft and space applications, is the occurrence of multiple fails. A major cause of this is the generation of multiple tracks by cosmic ray hits. This effect is modeled in a straight-forward manner since all tracks are considered in the generation of charge history files. In ref. [2] we have shown some of these calculations for a bipolar chip.

## IV. MODEL VS. EXPERIMENT

As mentioned before, we have considerable experimental verification of the model. In ref. [2] we have demonstrated the excellent agreement between SEMM predictions and the measurements for a radioactive alpha source of thorium placed on a bipolar chip. Here we present the data for protons and terrestrial cosmic rays. In Figure 11 we show the SEMM proton beam verification for a bipolar cache chip.

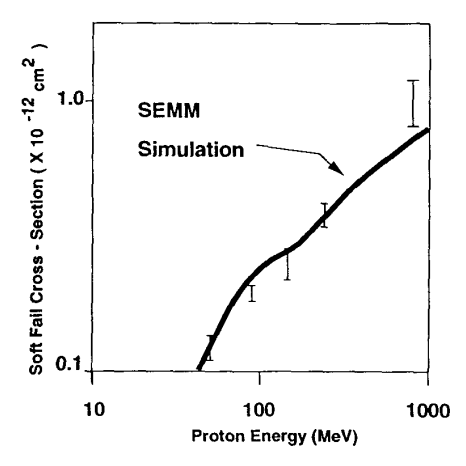


Fig.11. SEMM predictions vs. measurements of SEU rate due to protons at several energies for a bipolar chip.

In Table 2 we show similar proton measurements vs. SEMM predictions for many DRAM chips.

Chip SER (Relative Units)					
IC Chips	SEMM	Proton Beam			
1 Mbit DRAM	0.543	1.000			
4 Mbit DRAM	0.041	0.036			
16 Mbit DRAM	0.017	0.009			

Table 2. SEMM predictions vs. measurements of SEU rate due to 148 MeV protons for DRAMS of different densities.

The most convincing evidence that SEMM works well in predicting the SEU rate in actual computers due to terrestrial cosmic rays comes from the data shown in Table 3.

Chip SER (Relative Units)						
Altitude	SEMM (Model)	Field Test				
3.2 Km	21.0	19 - 27				
1.6 Km	6.8	5 - 8				
Sea Level	2.0					
200 m under ground	0	0				

Table 3. Cosmic ray SEU rate in a computer main frame tester - Model vs. Experiment.

For this data we are indebted to J.F.Ziegler et al. who took main frame testers to various locations in the Colorado mountains and into deep mines in Kansas. The fact that all these SEMM predictions were made without any parameter adjustments bears testimony to the predictiveness of the model.

## V. SOME CONCLUDING REMARKS

We have developed a SEU simulator which is predictive and parameter-free and one that can be used at the design stage of an IC chip. SEMM can be used to assess any part of the chip, such as memory cell, sense amps, bit lines, logic latches, etc. It allows computational experiments to find out, for example, what are the contributions of recoil nucleus vs. alpha particles in cosmic ray hits. One can use it to assess the funneling contribution vs. diffusion. We show such an example in Figure 12 for the relative contributions of recoils and alpha parti-

cles in a bipolar chip exposed to 90 MeV protons, as calculated by SEMM.

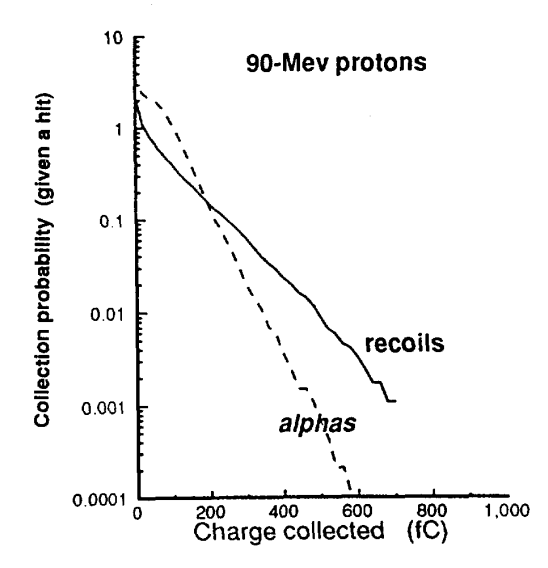


Fig.12. Calculated charge collection probabilities for alpha particles and recoils for a bipoar chip exposed to 90 MeV protons.

We see from the figure that for this chip geometry the recoils dominate the charge collection mechanism at high charge values, while the alphas are more prominent at low charges, mainly because of alpha multiplicity. As the chip size continues to shrink, one would expect the recoils to dominate the SEU rate, since the alpha track charge density may not be enough to deliver the critical charge in the small volume. This assumes that the critical charge stops tracking the feature size when a low, practical value of the critical charge has been reached for any given technology.

One can use SEMM to simulate ground rule scaling, technology changes due to SOI, buried implants, epi doping etc. It can also be used to simulate SEU rate in other semiconducting chips, such as GaAs. We would need diffusion and recombination parameters and energy loss tables for such a simulation. SEMM can be extended to space cosmic ray applications, since all the necessary charge collection, device-circuit and chip layout functions are in the simulator. We would need the radiation environment simulator which provides the radiation source input. Application to the case of primary protons in the near-earth environment is straightforward, since the proton-nucleus reactions are modeled already in NUSPA. The direct ionization effects of heavy ions in primary cosmic rays can also be simulated, if we know the stopping power of these ions along their tracks in the chip and the energyangle distributions of these heavy ions in space. However, modeling the strong interactions of the heavy ions with chip nuclei takes considerable ef-

The simulator presented in this paper was designed to be of practical use to chip designers who

are not specialists in the radiation field. One of their requirements is to be able to run the chip simulation in a reasonable cpu time and with memory available in to-day's work stations. Our IBM customers who ran this simulator for a wide variety of computer chips for several generations of bipolar and CMOS technologies have found that the design task can be accomplished in 20 to 30 hrs of cpu time for a full chip alpha particle and cosmic ray simulation. The memory requirements usually do not exceed 10 MB.

In summary, we have developed a powerful tool for SEU simulation which does not need any experimental inputs other than the chip layout and profiles and the relevant chip circuit model.

## **ACKNOWLEDGMENTS**

The soft error work at IBM is the outcome of a large effort by a number of people including the modeling people, experimental people, and chip designers. It is the result of several years of intensive work with close interactions between various groups. While it is not possible to acknowledge them individually, special thanks are due to Nestor Azziz, who helped in the initial nuclear physics formulations, Red O'Brien, Baji Gokhale, and Fred Astudillo for modeling assistance, Jim Ziegler and Hunt Curtis for the proton beam and mainframe tester measurements.

## REFERENCES

- [1] T.J. O'Gorman, "The Effect of Cosmic Rays on the Soft Errors of a DRAM at Ground Level" IEEE Trans. Electron Devices, Vol.41 pp. 533-557, 1994.
- [2] G.R. Srinivasan, P.C. Murley, and H.K. Tang, "Accurate, Predictive Modeling of Soft Error Rate due to Cosmic Rays and Chip Alpha Radiation" IEEE International Reliability Physics Symposium Proceedings, San Jose, CA, April 1994., pp. 12-16.
- [3] P.J. McNulty, W.G. Abdel-Kader, and J.E. Lynch, "Modeling Charge Collection and Single Event Upsets in Microelectronics", Nucl.Inst.Methods, Vol.B61, pp. 52-60, 1991.
- [4] E.L. Petersen, J.C. Pickel, J.H. Adams, and E.C. Smith, "Rate Prediction for Single Event Effects -- A Critique', IEEE Trans.Nucl.Sci. Vol.39, pp. 1577-1599, 1992.
- [5] M.A. Xapsos, "Applicability of LET to single events in Microelectronic Structures", IEEE Trans. Nucl. Sci., Vol. 39, pp. 1613-1621, 1992.
- [6] J.F. Ziegler and W.A. Lanford, "The Effect of Sea Level Cosmic Rays on Electronic Devices", J.Appl.Phys., Vol.52, pp. 4305-4312, 1981.
- [7] J.N. Bradford, "A Distribution Function for Ion Track Lengths in Rectangular Volumes", J.Appl.Phys., Vol.50, p. 3799, (1979).

- [8] E. Normand and W.R. Doherty, "Incorporation of ENDF-V Neutron Cross Section Data for Calculating Neutron Induced Single Event Upsets", IEEE Nucl.Sci., Vol.31, pp. 2349-2355, 1989.
- [9] J.R. Letaw and E. Normand, "Guide lines for Predicting Single Event Upsets in Neutron Environments", IEEE Trans.Nucl.Sci., Vol.38, pp. 1500-1506, 1991.
- [10] G.E. Farrel and P.J. McNulty, "Micro dosimetric Aspects of Proton Induced Nuclear Reactions in Thin Layers Of Silicon", IEEE Trans. Nucl.Sci., Vol. 29, p.2012, 1982.
- [11] S.S. Furkay and A.W. Strong, "3D Numerical Simulation of Prompt Charge Collection", 12th IBM Finite Element Modeling Conference, Almaden, CA, 1990.
- [12] H. Dussault, J.W. Howard, R.C. Block, M.R. Pinto, W.J. Stapor, and A.R. Knudson, "Numerical Simulation of Heavy Ion Charge Generation Collection Dynamics", IEEE Trans. Nucl.Sci., Vol. 40, pp. 1926-1934, 1993.
- [13] J.G. Rollins, T.K. Tsubota, W.A. Kolasinski, N.F. Haddad, L. Rockett, M. Cerilla, and W.B. Hennley, "Cost Effective, Numerical Simulation of SEU", IEEE Trans.Nucl.Sci., Vol.35, pp, 1608-1612, 1988.
- [14] R.L. Woodruff and P.J. Rudeck, "Three Dimensional Numerical Simulation of Single Event Upset of an SRAM Cell", IEEE Trans.Nucl.Sci., Vol.40, pp. 1795-1803, 1993.
- [15] S. Satoh, R. Sudo, H. Tashiro, N. Higaki, S. Yamaguchi, and N. Nakayama, "CMOS-SRAM Soft Error Simulation System", IEEE NUPAD V, pp. 181-184, 1994.
- [16] J.F. Ziegler, J.P. Biersack, and U. Littmark, The Stopping and Range of Ions in Solids, Vol. 1, Pergamon Press, 1985.
- [17] E.H. Auerbach, Brookhaven National Laboratory Report, BNL 6562. See Also: A. Bohr and B.R. Mottelson, Nuclear Structure Vol. I. Single-Particle Motion", W.A. Benjamin, Inc., 1969.
- [18] G.A. Sai-Halasz and M.R. Wordeman, "Monte Carlo Modeling of the Transport of Ionizing Radiation Created Carriers in Integrated Circuits", IEEE Electron Device Lett., Vol. EDL-10, pp. 211-213, 1980.
- [19] H.K. Tang, G.R. Srinivasan, and N. Azziz, "Cascade Statistical Model for Nucleon Induced Reactions on Light Nuclei in the Range 50 MeV 1 GeV", Phys.Rev.C, Vol. 42, pp. 1598-1622, 1990.
- [20] N. Azziz, H.K. Tang, and G.R. Srinivasan, "A Microscopic Model of Energy Deposition in Silicon Slabs exposed to High Energy Protons", Jour.Appl.Phys., Vol. 62, pp. 414-418, 1987.
- [21] H.W. Bertini, "Low-Energy Intranuclear Cascade Calculation", Phys.Rev. Vol. 131, pp. 1801-1821, 1963. See Also: Radiation Shielding Information Center Computer Code Documentation, "MECC-7, Medium Energy Intranuclear Cascade Code System", RSIC, Oak Ridge National Laboratory.